Applied Mathematics and Computation 207 (2009) 528–544

Contents lists available at ScienceDirect

Applied Mathematics and Computation

journal homepage: www.elsevier.com/locate/amc

Modeling and genetic algorithm optimization of early events in signal transduction via dynamics of G-protein-coupled receptors: Internalization consideration

Jeerapond Leelawattanachai [a,1], Charin Modchang [a,1], Wannapong Triampo [a,b,e,*], Darapond Triampo [a,c,e], Yongwimon Lenbury [d]

[a] R&D Group of Biological and Environmental Physics, Department of Physics, Faculty of Science, Mahidol University, Rama 6 Road, Ratchatewee, Bangkok 10400, Thailand
[b] Center of Excellence for Vector and Vector-Borne Diseases, Faculty of Science, Mahidol University, Nakhonpathom, Thailand
[c] Department of Chemistry, Faculty of Science, Mahidol University, Bangkok, Thailand
[d] Department of Mathematics, Faculty of Science, Mahidol University, Bangkok, Thailand
[e] Institute for Innovation and Development of Learning Process, Mahidol University, Bangkok, Thailand

ARTICLE INFO

Keywords:
Signal transduction
G-proteins
Receptors
Internalization
Mathematical model
Genetic algorithm

ABSTRACT

Signal transduction is the process of signal conversion that cells use to communicate among themselves and their environments. In this process, a cell converts one kind of signal or stimulus into another. This cellular communication brings about many cellular activities in response to the signals. Therefore, in-depth knowledge and understanding of this process, especially concerning the roles of G-proteins and cell receptors, which are the important components of the signal transduction process, could greatly benefit medical science, particularly in terms of medical diagnosis and treatment.

In this research we study early events in signal transduction including receptor/ligand binding and G-protein activation using an ordinary differential equation model. Motivated by experimental data and the mathematical model proposed by Chen et al. [C.Y. Chen et al., Modelling of signalling via G-protein coupled receptors: pathway-dependent agonist potency and efficacy, Bull. Math. Biol. 65 (2003) 933–958] to explain the agonist potency and efficacy of drugs regulated by signaling dynamics via G-proteins and receptors, we extended their model to take into account internalization, recycling, degradation and synthesis of the receptors in this process to obtain a more realistic model. By analyzing the extended model, we have found that the numerical results agree well with experimental observation. Qualitatively, this modified model is shown to be more realistic than the previous one in some respects when certain experimental findings are considered.

1. Introduction

Signal transduction is the process in which cells convert external signals, such as hormones, growth factors, neurotransmitters, and cytokines, to a specific internal cellular response, such as gene expression, cell division, or even apoptosis. This process begins at the cell membrane where an external stimulus initiates a cascade of enzymatic reactions inside the cell

* Corresponding author. Address: R&D Group of Biological and Environmental Physics, Department of Physics, Faculty of Science, Mahidol University, Rama 6 Road, Ratchatewee, Bangkok 10400, Thailand.
E-mail addresses: scwtr@mahidol.ac.th, wtriampo@gmail.com (W. Triampo).
[1] Co-first authors.

0096-3003/$ - see front matter © 2008 Elsevier Inc. All rights reserved.
doi:10.1016/j.amc.2008.11.008

that typically includes phosphorylation of proteins as mediators of downstream processes [1]. Signal transduction consists of three stages [2]. The first is *reception* – an agonist binds to a specific receptor on the cell membrane that triggers a change in the receptor molecule. The second is *transduction*. The change in the receptor brings about ordered sequences of biochemical reactions inside the cell that involve various enzymes, linked by second messengers. The third is *response*. After receiving the signal, target protein produces a response which can be any of many different cellular activities, such as activation of a certain enzyme, rearrangement of the cytoskeleton, or changes in gene expression. Receptors which possess seven-transmembrane domains that activate an intracellular effector system via the coupling of G-proteins (guanine nucleotide binding proteins) play a major role in transmembrane signal transduction [3,4]. G-protein-coupled receptors (GPCRs) constitute the largest family of cell surface receptors currently known [5], members of which are involved in all types of stimulus-response pathways, from intercellular communication to physiological senses. The diversity of functions is matched by the wide range of ligands recognized by members of the family. This pervasive involvement in normal biological processes has the consequence of involving GPCRs in many pathological conditions, which has led to GPCRs being the target of 40–50% of modern medicinal drugs [6].

In its inactive form, the heterotrimeric G-protein that couples to GPCR contains three different subunits α, β and γ. Of the three subunits, G_α subunit, the largest, binds to a GDP [7]. When an agonist binds to a GPCR on the exterior surface of the cell, the change in conformation of the receptor promotes the exchange of GDP for GTP on the G_α subunit, being presumed to allow the dissociation of the G_α and $G_{\beta\gamma}$ [8,9]. Subsequently, the activated G_α and/or $G_{\beta\gamma}$ exert their effect by binding to particular enzymes or other proteins in the cell. However, the activity of the G protein persists only as long as the G_α is bound to GTP and subunits remain separated. Eventually, the GTP-G_α subunit hydrolyzes its bound GTP, converting the subunit back to its inactive GDP-G_α form. Then, the inactive GDP-G_α subunit recombines with $G_{\beta\gamma}$ to form the inactive G heterotrimer [7]. In addition to receptor/ligand binding, under normal physiological conditions, dynamic trafficking events of receptors also occur in the signal transduction process concurrently with the binding [10]. These dynamic trafficking events consist of internalization, recycling, degradation and synthesis of receptors. In particular, cell surface receptors and receptor/ligand complexes can be internalized in a process known as receptor-mediated endocytosis (RME) [10]. Receptors and receptor/ligand complexes can accumulate, most likely by diffusion in the plasma membrane followed by trapping, in localized membrane regions on the cell surface – called pits. Internalization of receptors occurs when pits, which receptors and/or complexes congregate within, invaginate and pinch off to form intracellular vesicles. Then the vesicular contents accumulate in large intracellular organelles called endosomes. Within endosomes, receptors and complexes may be sorted to have at least two possible fates: recycling to the cell surface or degradation in lysosomes. Due to degradation, the cell can decrease the number of cell surface receptors and therefore its ability to respond to future doses of the same ligand. Thus, it is necessary for the cell to synthesize new receptors and deliver them to the cell surface.

Focusing on the one step G-protein activation models and the assumption that receptors and G-proteins can move freely within the cell membrane, extensive mathematical models have been constructed and modified in the past to account for the role of GPCRs in signal transduction. De Lean et al. [11] proposed the ternary complex model (TCM), in which the receptors are allowed to interact with G-protein as well as ligands. Several studies (see, for example, [12,13]) have shown that under certain conditions, sufficient concentrations of receptors are present in the activated state under basal conditions, producing a response in the absence of agonist – called constitutive receptor activity. To account for constitutive activities, the extended ternary complex model (eTCM) [14] and the cubic ternary complex model (CTC) [15,16] were proposed. Some receptors can couple to more than one G-protein subtype, activating multiple signaling pathways (see, for example, [12,13,17,18]). Agonists may express multiple efficacies and exhibit different agonist potency for different effector pathways when coupled to a single receptor type, depending on the response being measured. Note that efficacy is defined as the maximum response induced by the agonist and potency is a measure of the concentration of a drug required for it to be effective and is often defined as the drug concentration that induces half of the maximum response, either activation or inhibition (denoted by $EC50$ or $IC50$, respectively). Many mathematical models have been proposed to describe these events, for example the equilibrium models of Weiss et al. [15,16] and Leff et al. [19] and the ordinary differential equation models of Riccobene et al. [20] and Chen et al. [3]. The multiple receptor active conformations model of Chen et al. [3] demonstrates the role of G-proteins in determining pathway-dependent agonist potency. The model is based on the possibility of agonist-directed trafficking, allowing the constitutive activities in the absence of any ligand, and two assumptions that the distribution of receptors and G-proteins is uniform throughout and G-protein activation is considered as a one-step process. However, Chen et al. [3] neglected receptor trafficking, specifically receptor internalization which normally takes place in a signal transduction process [10] and occurs rapidly when GPCRs are exposed to agonists [5]. Therefore, it should be more realistic to extend their model to take into account the dynamic trafficking events of the receptors, consisting of internalization, recycling, degradation and synthesis.

Due to the fact that there is a considerable amount of pharmacological research in which consideration is focused on efficacy and potency of drugs, steady-state or quasi-steady-state analysis is imperative for elucidation of the results in order to gain better understanding of the processes. At steady-state, the concentrations and numbers of all species in the system remain constant. These steady-state values are crucial values which are directly related to efficacy and can be used to determine potency. Moreover, in some cases the time scale for the response in signal transduction process is very short and the measurement procedures can require a few seconds to a few minutes [10]. In these situations, those experimental results cannot be measured easily at non-steady-state. Hence, steady-state consideration seem to be a good solution for studying signal transduction in these cases.

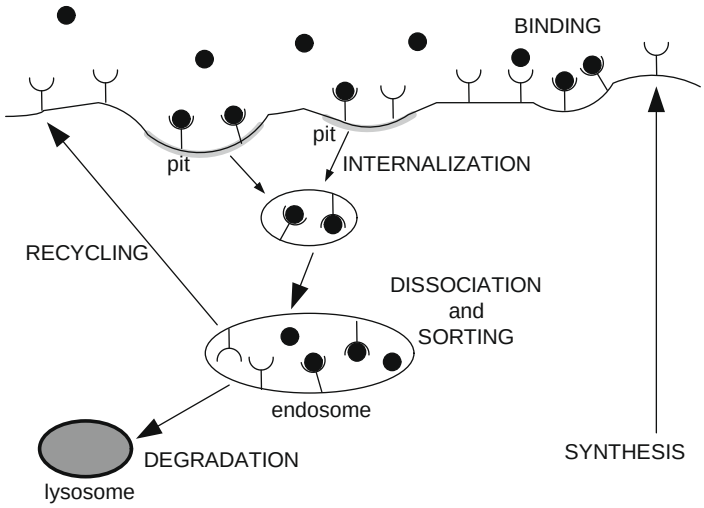

Fig. 1. Dynamic trafficking of receptors. The idea is based on Ref. [10].

Upon construction of a mathematical model, the model parameters often are only partially known. This implies that model approximations and numerical estimates and, whenever possible, additional specific experimental measurements are necessary to make a numerical simulation feasible and reliable. To estimate parameters, there are many different kinds of global optimization methods including both calculus and non-calculus based optimization [21,22]. Evolutionary computation (EC), also known as biologically inspired methods, or population-bases stochastic methods, is a very popular class of methods based on the ideas of biological evolution, which is driven by the mechanisms of reproduction, mutation, and the principle of survival of the fittest [23]. Similarly to biological evolution, evolutionary computing methods generate better and better solutions by iteratively creating new "generations" by means of those mechanisms in numerical form. EC methods are usually classified into three groups: Genetic algorithms (GAs), evolutionary programming (EP) and evolution strategies (ES). Up to date, GAs are by far the most popular EC methods [23].

In the present work, by modifying the model of Chen et al. [3], we propose a mathematical model to investigate the dynamics of GPCRs, considering receptor internalization, recycling, degradation and synthesis. Our model still has three G-protein subtypes. The number of G-protein subtypes in the real biological system can be very different depending on what system we are dealing with. Here we are aiming to explain the experimental data from Ref. [13] by extending the model from Ref. [3]. Both Refs. [10,13] did experiments on a biological system which has three G-protein subtypes, so our model has to have three subtypes of G-protein to make this particular model consistent with the experimental data. We have estimated a set of the model parameters by using the genetic algorithm and the experimental results obtained by Cordeaux et al. [13], who studied the effects of varying the total number of receptors on the maximum response, on the intrinsic activities and the potency order of agonist along separate pathways and on the observed pathway-dependent changes in agonist potency. These parameters have been assessed to be relevant for the reproduction of the available experimental data and their values can also help to clarify the dynamics of GPCRs (see Fig. 1).

2. The mathematical model

2.1. Formulation of the problem

We extended the multi receptor active conformations model of Chen et al. [3] by taking into account internalization, recycling, degradation and synthesis of GPCRs. In our model, as shown diagrammatically in Fig. 2, there are three G-protein subtypes whose numbers will be denoted by G_j, when $j = 1,2,3$. The input and output signals for this model are an agonist (A) and activated G-proteins (G_j^*), respectively, when $j = 1,2,3$. In the absence of any agonist (A), the receptor is hypothesized to exist in four states, an inactive conformation (R) and three active conformations (R^{i^*}), each interacting with a specific G-protein subtype. Under basal conditions, the inactive receptor (R) can convert into an active state (R^{i^*}) with rate constant L_j^+, and from the active back to the inactive state with rate constant L_j^-. When the receptors are exposed to agonists, both inactive receptors (R) and three types of active receptors (R^{i^*}) can be bound to be ligand-bound receptors (R_A) and activated ligand-bound receptors (R_A^*). Rate constants of inactive receptor (R)/ligand (A) binding and dissociating are K^+ and K^-, respectively, and the parameters μ_j represent the effect of the ligand on receptor activation, corresponding to the various G_j-linked pathways. For example, an agonist may exhibit high preference for a particular pathway, namely G_1, such that $\mu_1 \gg \mu_2, \mu_3$, increasing the population of receptors coupled to this G-protein, reducing that of other active conformations. The effect of the agonist is felt by slowing down the ligand off-rate, K^-/μ_j, from the ligand-bound activated receptors ($R_A^{i^*}$) and, consequently, the backward conversion rate from $R_A^{i^*}$ to R_A is L_j^-/μ_j.

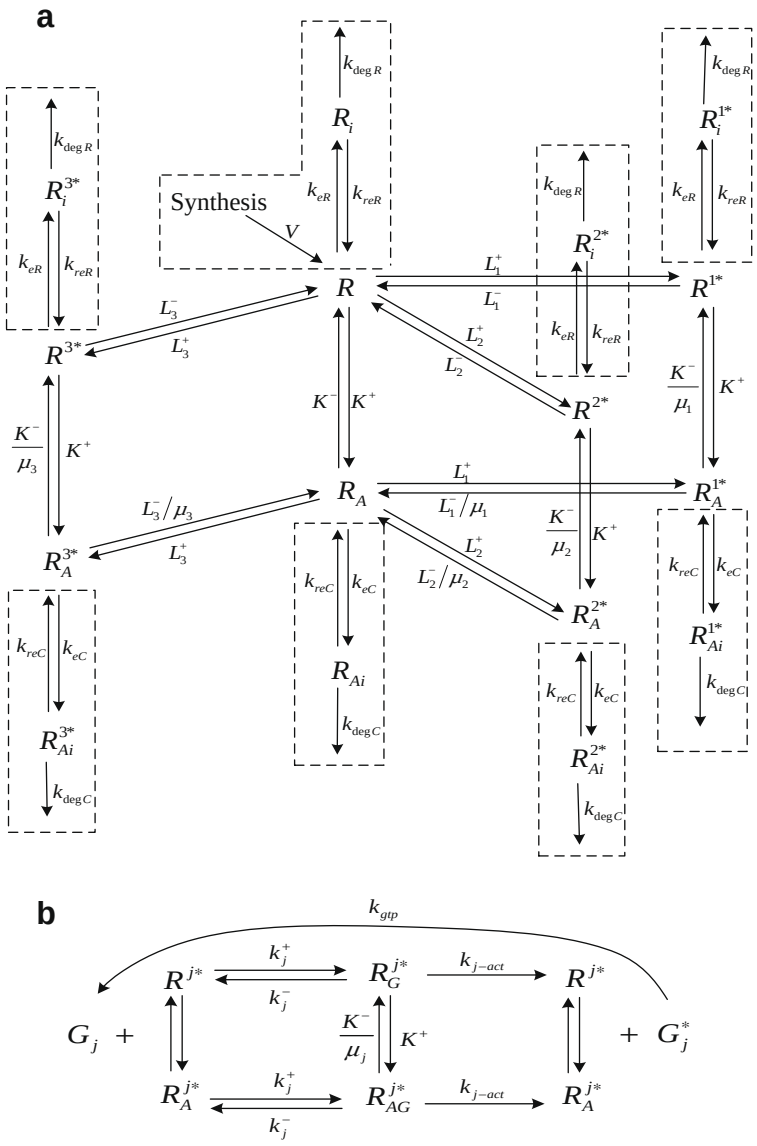

Fig. 2. Model structure of (a) receptor/ligand binding and receptor trafficking with multiple receptor conformations; (b) G-protein activation of the G_j-linked pathway, assuming R^* and R_A^* associate with and dissociate from G-protein at the same rate. Model structures (a) and (b) are coupled together in the positions of R^{j^*} and $R_A^{j^*}$, when $j = 1,2,3$. The added model parameters concerning dynamic trafficking events of receptors are enclosed by dashed-line boxes. Note that ligands (A), which interact with R and R^{j^*} are not shown in this figure.

Rate constants describing the internalization of both the active forms and inactive form of free receptors (R, R^{j^*}) and receptor/ligand complexes ($R_A, R_A^{j^*}$) are k_{eR} and k_{eC} in respective order. Allowing these to be different reflects the possible selectivity of endocytosis for receptor states. V is the rate of new receptor synthesis and expression on the cell surface as free receptors only in the inactive form (R). k_{reR} and k_{reC} represent the rate constants for transport of internalized free receptors ($R_i, R_i^{j^*}$) and complexes ($R_{Ai}, R_{Ai}^{j^*}$), respectively, via vesicle from the endosome back to the cell surface – recycling. $k_{\deg R}$ and $k_{\deg C}$ represent lumped rate constants for the routing of internalized free receptors ($R_i, R_i^{j^*}$) and complexes ($R_{Ai}, R_{Ai}^{j^*}$) from the endosome to the lysosome, degradation in the lysosome and the release of fragments in the extracellular medium.

As depicted in Fig. 2b, the activated receptors, with or without bound ligand ($R^{j^*}, R_A^{j^*}$), associate with and dissociate from G-protein with rate constants k_j^+ and k_j^- for G_j. The symbols $R_G^{j^*}$ and $R_{AG}^{j^*}$ denote the number of G_j-coupled active receptors and that of ligand–receptor-G_j complexes, respectively. Both G-protein activation and inactivation are assumed as one-step processes with rate constants k_{j-act} and k_{gtp}. In this model, we consider that only GTP-bound G_α subunits (and not $G_{\beta\gamma}$) are the activated G-proteins – output signals.

Model structures in parts (a) and (b) in Fig. 2 are coupled together in the positions of R^{j^*} and $R_A^{j^*}$, when $j = 1,2,3$.

The important feature of our model is the added parameters concerning dynamic trafficking events of receptors. The parameters consist of $R_i, R_i^{j^*}, R_{Ai}, R_{Ai}^{j^*}, k_{eR}, k_{eC}$ – internalization; k_{reR},k_{reC} – recycling; $k_{\deg R}$,$k_{\deg C}$ – degradation; V-synthesis. The added parameters are enclosed by dashed-line boxes as shown in Fig. 2.

From the diagram shown in Fig. 2 and based on the principles of mass action kinetics and the assumption that the total number of receptors and that of each G-protein subtype on the cell surface and the concentration of ligand (A) remain constant throughout the interaction, the system of equations can be derived as follows:

$$\frac{dR}{dt} = \sum_{n=1}^{3} L_n^- R^{n^*} + K^- R_A - \left(\sum_{n=1}^{3} L_n^+ + K^+ A\right) R - k_{eR} R + k_{reR} R_i + V, \tag{2.1}$$

$$\frac{dR^{j^*}}{dt} = \frac{K^-}{\mu_j} R_A^{j^*} + L_j^+ R - (L_j^- + K^+ A) R^{j^*} - k_{eR} R^{j^*} + k_{reR} R_i^{j^*} - k_j^+ G_j R^{j^*} + (k_j^- + k_{j\text{-}act}) R_G^{j^*}, \tag{2.2}$$

$$\frac{dR_A^{j^*}}{dt} = K^+ A R^{j^*} + L_j^+ R_A - \left(\frac{L_j^-}{\mu_j} + \frac{K^-}{\mu_j}\right) R_A^{j^*} - k_{eC} R_A^{j^*} + k_{reC} R_{Ai}^{j^*} - k_j^+ G_j R_A^{j^*} + (k_j^- + k_{j\text{-}act}) R_{AG}^{j^*}, \tag{2.3}$$

$$\frac{dR_i}{dt} = k_{eR} R - (k_{reR} + k_{\deg R}) R_i, \tag{2.4}$$

$$\frac{dR_i^{j^*}}{dt} = k_{eR} R^{j^*} - (k_{reR} + k_{\deg R}) R_i^{j^*}, \tag{2.5}$$

$$\frac{dR_{Ai}}{dt} = k_{eC} R_A - (k_{reC} + k_{\deg C}) R_{Ai}, \tag{2.6}$$

$$\frac{dR_{Ai}^{j^*}}{dt} = k_{eC} R_A^{j^*} - (k_{reC} + k_{\deg C}) R_{Ai}^{j^*}, \tag{2.7}$$

$$\frac{dR_{AG}^{j^*}}{dt} = k_j^+ G_j R_A^{j^*} - (k_j^- + k_{j\text{-}act}) R_{AG}^{j^*} + K^+ A R_G^{j^*} - \frac{K^-}{\mu_j} R_{AG}^{j^*}, \tag{2.8}$$

$$\frac{dR_G^{j^*}}{dt} = k_j^+ G_j R^{j^*} - (k_j^- + k_{j\text{-}act}) R_G^{j^*} - K^+ A R_G^{j^*} + \frac{K^-}{\mu_j} R_{AG}^{j^*}, \tag{2.9}$$

$$\frac{dG_j^*}{dt} = k_{j\text{-}act}(R_G^{j^*} + R_{AG}^{j^*}) - k_{gtp} G_{\beta\gamma} G_j^*, \tag{2.10}$$

where

$$\begin{aligned} G_{\beta\gamma} &= G_1^* + G_2^* + G_3^*, \\ R_A &= R_0 - R - R_i - R_{Ai} - \sum_{n=1}^{3} (R^{n^*} + R_A^{n^*} + R_i^{n^*} + R_{Ai}^{n^*} + R_{AG}^{n^*} + R_G^{n^*}), \\ G_j &= g_j - G_j^* - R_{AG}^{j^*} - R_G^{j^*} \end{aligned} \tag{2.11}$$

with g_j's and R_0 constant. Here, we adopt the assumption that the numbers of receptors and G-proteins in the system are conserved as in the work of Chen et al. [3]. Although in our case receptor synthesis and degradation are also considered, the net change in the total number of receptors are still very small. We therefore believe that the assumption on receptor and G-protein conservation is still valid.

2.2. Nondimensionalization

We now nondimensionalize the system of Eqs. (2.1)–(2.10) and (2.11) by the rescaling

$$\begin{aligned} &t = T\bar{t}, \quad R = R_0 \bar{R}, \quad R^{j^*} = R_0 \bar{R}^{j^*}, \quad R_A^{j^*} = R_0 \bar{R}_A^{j^*}, \\ &R_i = R_0 \bar{R}_i, \quad R_i^{j^*} = R_0 \bar{R}_i^{j^*}, \quad R_{Ai} = R_0 \bar{R}_{Ai}, \quad R_{Ai}^{j^*} = R_0 \bar{R}_{Ai}^{j^*}, \\ &R_{AG}^{j^*} = R_0 \bar{R}_{AG}^{j^*}, \quad R_G^{j^*} = R_0 \bar{R}_G^{j^*}, \quad R_A = R_0 \bar{R}_A, \quad A = a_0 \bar{A}, \\ &G_j = G_0 \bar{G}_j, \quad G_j^* = G_0 \bar{G}_j^*, \quad g_j = G_0 \bar{g}_j, \quad G_{\beta\gamma} = G_0 \bar{G}_{\beta\gamma}, \end{aligned} \tag{2.12}$$

where $G_0 = g_1 + g_2 + g_3$, and thus $\bar{g}_1 + \bar{g}_2 + \bar{g}_3 = 1$. While the ligand concentration (A) remains constant throughout each interaction, it is convenient for the purpose of drawing the concentration-response curve (which is the result of various interactions, each with a different ligand concentration), to rescale A by a given, representative, concentration a_0 rather than scaling such that $\bar{A} = 1$. The dimensionless quantity $\bar{A}$ is treated as a parameter in the analysis which follows. We nondimensionalize the reactions, which occur in accordance with the diagram in Fig. 2a, letting by

$$T = \frac{1}{K^-}, \quad \bar{K}^+ = \frac{K^+ a_0}{K^-}, \quad \bar{L}_j^+ = \frac{L_j^+}{K^-}, \quad \bar{L}_j^- = \frac{L_j^-}{K^-}, \quad \bar{V} = \frac{V}{R_0 K^-},$$
$$\bar{k}_{eR} = \frac{k_{eR}}{K^-}, \quad \bar{k}_{reR} = \frac{k_{reR}}{K^-}, \quad \bar{k}_{\deg R} = \frac{k_{\deg R}}{K^-},$$
$$\bar{k}_{eC} = \frac{k_{eC}}{K^-}, \quad \bar{k}_{reC} = \frac{k_{reC}}{K^-}, \quad \bar{k}_{\deg C} = \frac{k_{\deg C}}{K^-}. \tag{2.13}$$

In general, the binding of G-protein to an activated receptor leads to the activation of the G-protein and thus the dissociation rate constant k_j^- is assumed very small and $k_{j\text{-}act} \gg k_{gtp} G_0, k_j^+ G_0$ (based on the supposition that the amount of G-proteins available in the system is moderate). We now make such assumptions more precise and nondimensionalize the parameters for receptor and G-protein association/dissociation, the release of activated G_α subunits and the hydrolysis of GTP, in order to revert to the inactive state (as shown diagrammatically in Fig. 2b) by setting

$$\varepsilon = \frac{K^-}{k_{1-act}}, \quad \frac{\bar{k}_{j\text{-}act}}{\varepsilon} = \frac{k_{j\text{-}act}}{K^-}, \quad \varepsilon \bar{k}_j^- = \frac{k_j^-}{K^-},$$
$$\bar{k}_{gtp} = \frac{k_{gtp}}{K^-} G_0, \quad \bar{k}_j^+ = \frac{k_j^+}{K^-} G_0, \tag{2.14}$$

where

$$\bar{k}_j^- = \frac{k_j^- k_{1-act}}{(K^-)^2}, \quad \bar{k}_{j\text{-}act} = \frac{k_{j\text{-}act}}{k_{1-act}}, \quad \bar{k}_{1-act} = 1. \tag{2.15}$$

After rewriting the system of equation in terms of the nondimensionalized variables and dropping the overbars henceforth for brevity, the nondimensionalized system of equations is then

$$\frac{dR}{dt} = \sum_{n=1}^{3} L_n^- R^{n^*} + R_A - \left(\sum_{n=1}^{3} L_n^+ + K^+ A \right) R - k_{eR} R + k_{reR} R_i + V, \tag{2.16}$$

$$\frac{dR^{j^*}}{dt} = L_j^+ R + \frac{1}{\mu_j} R_A^{j^*} - (L_j^- + K^+ A) R^{j^*} - k_{eR} R^{j^*} + k_{reR} R_i^{j^*} - k_j^+ G_j R^{j^*} + \left(\varepsilon k_j^- + \frac{k_{j\text{-}act}}{\varepsilon} \right) R_G^{j^*}, \tag{2.17}$$

$$\frac{dR_A^{j^*}}{dt} = K^+ A R^{j^*} + L_j^+ R_A - \left(\frac{L_j^-}{\mu_j} + \frac{1}{\mu_j} \right) R_A^{j^*} - k_{eC} R_A^{j^*} + k_{reC} R_{Ai}^{j^*} - k_j^+ G_j R_A^{j^*} + \left(\varepsilon k_j^- + \frac{k_{j\text{-}act}}{\varepsilon} \right) R_{AG}^{j^*}, \tag{2.18}$$

$$\frac{dR_i}{dt} = k_{eR} R - (k_{reR} + k_{\deg R}) R_i, \tag{2.19}$$

$$\frac{dR_i^{j^*}}{dt} = k_{eR} R^{j^*} - (k_{reR} + k_{\deg R}) R_i^{j^*}, \tag{2.20}$$

$$\frac{dR_{Ai}}{dt} = k_{eC} R_A - (k_{reC} + k_{\deg C}) R_{Ai}, \tag{2.21}$$

$$\frac{dR_{Ai}^{j^*}}{dt} = k_{eC} R_A^{j^*} - (k_{reC} + k_{\deg C}) R_{Ai}^{j^*}, \tag{2.22}$$

$$\frac{dR_{AG}^{j^*}}{dt} = k_j^+ G_j R_A^{j^*} - \left(\varepsilon k_j^- + \frac{k_{j\text{-}act}}{\varepsilon} \right) R_{AG}^{j^*} + K^+ A R_G^{j^*} - \frac{1}{\mu_j} R_{AG}^{j^*}, \tag{2.23}$$

$$\frac{dR_G^{j^*}}{dt} = k_j^+ G_j R^{j^*} - \left(\varepsilon k_j^- + \frac{k_{j\text{-}act}}{\varepsilon} \right) R_G^{j^*} - K^+ A R_G^{j^*} + \frac{1}{\mu_j} R_{AG}^{j^*}, \tag{2.24}$$

$$\frac{dG_j^*}{dt} = N \frac{k_{j\text{-}act}}{\varepsilon} (R_G^{j^*} + R_{AG}^{j^*}) - k_{gtp} G_{\beta\gamma} G_j^* \tag{2.25}$$

and

$$R_A = 1 - R - R_i - R_{Ai} - \sum_{n=1}^{3} (R^{n^*} + R_A^{n^*} + R_i^{n^*} + R_{Ai}^{n^*} + R_{AG}^{n^*} + R_G^{n^*}),$$
$$G_j = g_j - G_j^* - N R_{AG}^{j^*} - N R_G^{j^*} \tag{2.26}$$

for $j = 1,2,3$ and $N = R_0/G_0$. The initial conditions are $R = 1$, $G_j = g_j$ with $g_1 + g_2 + g_3 = 1$, with the other species having zero concentrations. Note that we have assumed that the concentration ratio of the receptors and G-proteins is $N = R_0/G_0$.

From Eqs. (2.23) and (2.24), the scaling implies that $R^{j^*}_{AG}, R^{j^*}_{G} = O(\varepsilon)$ in fact holds, so that these quantities should be rescaled. By writing $R^{j^*}_{AG} = \varepsilon \widetilde{R}^{j^*}_{AG}$ and $R^{j^*}_{G} = \varepsilon \widetilde{R}^{j^*}_{G}$, Eqs. (2.23)–(2.25) and (2.26) thus become

$$\frac{d\widetilde{R}^{j^*}_{AG}}{dt} = \frac{k_j^+}{\varepsilon} G_j R^{j^*}_{A} - \left(\varepsilon k_j^- + \frac{k_{j\text{-}act}}{\varepsilon}\right)\widetilde{R}^{j^*}_{AG} + K^+ A \widetilde{R}^{j^*}_{G} - \frac{1}{\mu_j}\widetilde{R}^{j^*}_{AG}, \tag{2.27}$$

$$\frac{d\widetilde{R}^{j^*}_{G}}{dt} = \frac{k_j^+}{\varepsilon} G_j R^{j^*} - \left(\varepsilon k_j^- + \frac{k_{j\text{-}act}}{\varepsilon}\right)\widetilde{R}^{j^*}_{G} - K^+ A \widetilde{R}^{j^*}_{G} + \frac{1}{\mu_j}\widetilde{R}^{j^*}_{AG}, \tag{2.28}$$

$$\frac{dG^*_j}{dt} = N k_{j\text{-}act}(\widetilde{R}^{j^*}_{G} + \widetilde{R}^{j^*}_{AG}) - k_{gtp} G_{\beta\gamma} G^*_j \tag{2.29}$$

and

$$\begin{aligned} R_A &= 1 - R - R_i - R_{Ai} - \sum_{n=1}^{3}(R^{n^*} + R^{n^*}_{A} + R^{n^*}_{i} + R^{n^*}_{Ai} + \varepsilon\widetilde{R}^{n^*}_{AG} + \varepsilon\widetilde{R}^{n^*}_{G}), \\ G_j &= g_j - G^*_j - \varepsilon N \widetilde{R}^{j^*}_{AG} - \varepsilon N \widetilde{R}^{j^*}_{G}. \end{aligned} \tag{2.30}$$

2.3. Quasi-steady state analysis

A quasi-steady state is a situation in which some state variables are approximately constant. Therefore, at the quasi-steady state the concentrations and numbers of some of the species in our system remain approximately constant; consequently their time derivatives are extremely small. In the limit $\varepsilon \to 0$, Eqs. (2.27) and (2.28) become quasi-steady, i.e., to leading order they imply

$$\widetilde{R}^{j^*}_{AG} = \frac{k_j^+ G_j}{k_{j\text{-}act}} R^{j^*}_{A}, \quad \widetilde{R}^{j^*}_{G} = \frac{k_j^+ G_j}{k_{j\text{-}act}} R^{j^*}. \tag{2.31}$$

Using (2.31) to eliminate $R^{j^*}_{AG}$ and $R^{j^*}_{G}$ from (2.17), (2.18) and (2.29) enables these equations to be expressed as follows:

$$\frac{dR^{j^*}}{dt} = L_j^+ R + \frac{1}{\mu_j} R^{j^*}_{A} - (L_j^- + K^+ A) R^{j^*} - k_{eR} R^{j^*} + k_{reR} R^{j^*}_{i}, \tag{2.32}$$

$$\frac{dR^{j^*}_{A}}{dt} = K^+ A R^{j^*} + L_j^+ R_A - \left(\frac{L_j^-}{\mu_j} + \frac{1}{\mu_j}\right) R^{j^*}_{A} - k_{eC} R^{j^*}_{A} + k_{reC} R^{j^*}_{Ai}, \tag{2.33}$$

$$\frac{dG^*_j}{dt} = N k_j^+ G_j (R^{j^*}_{A} + R^{j^*}) - k_{gtp} G_{\beta\gamma} G^*_j. \tag{2.34}$$

At steady-state, Eq. (2.34) can be rewritten as

$$N k_j^+ G_j (R^{j^*}_{A} + R^{j^*}) - k_{gtp} G_{\beta\gamma} G^*_j = 0. \tag{2.35}$$

When $\epsilon \to 0$, Eq. (2.30) becomes

$$\begin{aligned} R_A &= 1 - R - R_i - R_{Ai} - \sum_{n=1}^{3}(R^{n^*} + R^{n^*}_{A} + R^{n^*}_{i} + R^{n^*}_{Ai}), \\ G_j &= g_j - G^*_j. \end{aligned} \tag{2.36}$$

We now substitute the second equality in Eq. (2.36) into Eq. (2.35) to obtain

$$G^*_j = \frac{H_j g_j}{1 + H_j},$$

when

$$H_j \equiv \frac{N k_j^+}{k_{gtp} G_{\beta\gamma}} (R^{j^*}_{A} + R^{j^*}). \tag{2.37}$$

We now summarize the overall equations from the results of the quasi-steady state analysis as follows:

$$\frac{dR}{dt} = \sum_{n=1}^{3} L_n^- R^{n^*} + R_A - \left(\sum_{n=1}^{3} L_n^+ + K^+ A\right) R - k_{eR} R + k_{reR} R_i + V, \tag{2.38}$$

$$\frac{dR^{j^*}}{dt} = L_j^+ R + \frac{1}{\mu_j} R_A^{j^*} - (L_j^- + K^+ A) R^{j^*} - k_{eR} R^{j^*} + k_{reR} R_i^{j^*}, \tag{2.39}$$

$$\frac{dR_A^{j^*}}{dt} = K^+ A R^{j^*} + L_j^+ R_A - \left(\frac{L_j^-}{\mu_j} + \frac{1}{\mu_j}\right) R_A^{j^*} - k_{eC} R_A^{j^*} + k_{reC} R_{Ai}^{j^*}, \tag{2.40}$$

$$\frac{dR_i}{dt} = k_{eR} R - (k_{reR} + k_{\deg R}) R_i, \tag{2.41}$$

$$\frac{dR_i^{j^*}}{dt} = k_{eR} R^{j^*} - (k_{reR} + k_{\deg R}) R_i^{j^*}, \tag{2.42}$$

$$\frac{dR_{Ai}}{dt} = k_{eC} R_A - (k_{reC} + k_{\deg C}) R_{Ai}, \tag{2.43}$$

$$\frac{dR_{Ai}^{j^*}}{dt} = k_{eC} R_A^{j^*} - (k_{reC} + k_{\deg C}) R_{Ai}^{j^*}, \tag{2.44}$$

where

$$R_A = 1 - R - R_i - R_{Ai} - \sum_{n=1}^{3} (R^{n^*} + R_A^{n^*} + R_i^{n^*} + R_{Ai}^{n^*}),$$

$$G_j = g_j - G_j^* \tag{2.45}$$

and

$$G_j^* = \frac{H_j g_j}{1 + H_j},$$

when

$$H_j \equiv \frac{N k_j^+}{k_{gtp} G_{\beta\gamma}} (R_A^{j^*} + R^{j^*}). \tag{2.46}$$

The analysis above can be summarized as follows. Firstly, based on the assumption that each protein species would reach steady state with different timescales, we thus set some equations equal zero i.e., (2.27), (2.28) and (2.34). With this way we can reduce the numbers of equation from 10 to 7 ODEs. This is the main reason why we called quasi-steady state (not all equations in the system reach steady state) which might not be quite appropriate term. Then, we transform the system of equations into finite difference form. Since it is very time consuming for each generation of getting parameters via genetic algorithm, we did not directly apply numerical integration process to find the steady state values of optimized parameters. We instead applied the theorem of geometric series for matrices for finding steady state variables or measurements corresponding to each estimated parameter set (in that generation). These steady state variables will then be used for finding the fitness function. This process is repeated until we obtain the optimal parameters.

2.4. Steady-state solutions

In order to explain the experimental results obtained in the work of Cordeaux et al. [13], in which measurements were made after the experiment had been running for a sufficiently long time that steady-state conditions could be assumed. By using the theorem on geometric series for matrices [24] to find the steady-state solutions, we first transform the model equations, after our quasi-steady state analysis, into the matrix form. We replace the derivative $\frac{dy}{dt}$ (where y refers to each of our variables: $R, R^{j^*}, R_A^{j^*}, R_i, R_i^{j^*}, R_{Ai}, R_{Ai}^{j^*}$) by the finite difference approximation

$$\frac{dy}{dt} \approx \frac{y(t + \Delta t) - y(t)}{\Delta t},$$

which yields the following formula:

$$y(t + \Delta t) \approx y(t) + \Delta t(f(t, y(t))), \tag{2.47}$$

when the step size Δt should be very small. Then, we construct the sequence $t_0, t_1 = t + \Delta t, t_2 = t + 2(\Delta t), \ldots$, in which y_n denotes numerical estimate of the exact solution $y(t_n)$. Motivated by (2.47), we compute this estimate by the following recursive scheme:

$$y_{n+1} = y_n + \Delta t(f(t_n, y_n)). \tag{2.48}$$

Then, we write these finite-difference equations in the matrix form as

$$u^{k+1} = Du^k + b. \tag{2.49}$$

Here, u^{k+1} is a sequence of column vectors, which represents the number of each type of receptors at time step $k+1$. In the current work, our system of equations in the matrix form is represented by (2.49) when

$$u = \begin{bmatrix} R \\ R^{1*} \\ R^{2*} \\ R^{3*} \\ R_A^{1*} \\ R_A^{2*} \\ R_A^{3*} \\ R_i \\ R_i^{1*} \\ R_i^{2*} \\ R_i^{3*} \\ R_{Ai} \\ R_{Ai}^{1*} \\ R_{Ai}^{2*} \\ R_{Ai}^{3*} \end{bmatrix}, \quad b = \begin{bmatrix} V+1 \\ 0 \\ 0 \\ 0 \\ L_1^+ \\ L_2^+ \\ L_3^+ \\ 0 \\ 0 \\ 0 \\ 0 \\ k_{ec} \\ 0 \\ 0 \\ 0 \end{bmatrix} \Delta t$$

and

$$D_1 = \begin{bmatrix} \left\{\frac{1}{\Delta t} - \sum L_n^+ - K^+A - 1 - k_{eR}\right\} & L_1^- - 1 & L_2^- - 1 & L_3^- - 1 & -1 & -1 & -1 \\ k_{reR} - 1 & -1 & -1 & -1 & -1 & -1 & -1 & -1 \end{bmatrix}\Delta t,$$

$$D_2 = \begin{bmatrix} L_1^+ & \left\{\frac{1}{\Delta t} - L_1^- - K^+A - k_{eR}\right\} & 0 & 0 & \frac{1}{\mu_1} & 0 & 0 & 0 & k_{reR} & 0 & 0 & 0 & 0 & 0 & 0 \end{bmatrix}\Delta t,$$

$$D_3 = \begin{bmatrix} L_2^+ & 0 & \left\{\frac{1}{\Delta t} - L_2^- - K^+A - k_{eR}\right\} & 0 & 0 & \frac{1}{\mu_2} & 0 & 0 & 0 & k_{reR} & 0 & 0 & 0 & 0 & 0 \end{bmatrix}\Delta t,$$

$$D_4 = \begin{bmatrix} L_3^+ & 0 & 0 & \left\{\frac{1}{\Delta t} - L_3^- - K^+A - k_{eR}\right\} & 0 & 0 & \frac{1}{\mu_3} & 0 & 0 & 0 & k_{reR} & 0 & 0 & 0 & 0 \end{bmatrix}\Delta t,$$

$$D_5 = \begin{bmatrix} -L_1^+ & K^+A - L_1^+ & -L_1^+ & -L_1^+ & \left\{\frac{1}{\Delta t} - \frac{L_1^-}{\mu_1} - \frac{1}{\mu_1} - k_{eC} - L_1^+\right\} & -L_1^+ & -L_1^+ \\ -L_1^+ & -L_1^+ & -L_1^+ & -L_1^+ & -L_1^+ & k_{reC} - L_1^+ & -L_1^+ & -L_1^+ \end{bmatrix}\Delta t,$$

$$D_6 = \begin{bmatrix} -L_2^+ & -L_2^+ & K^+A - L_2^+ & -L_2^+ & -L_2^+ & \left\{\frac{1}{\Delta t} - \frac{L_2^-}{\mu_2} - \frac{1}{\mu_2} - k_{eC} - L_2^+\right\} & -L_2^+ \\ -L_2^+ & -L_2^+ & -L_2^+ & -L_2^+ & -L_2^+ & k_{reC} - L_2^+ & -L_2^+ \end{bmatrix}\Delta t,$$

$$D_7 = \begin{bmatrix} -L_3^+ & -L_3^+ & -L_3^+ & K^+A - L_3^+ & -L_3^+ & -L_3^+ & \left\{\frac{1}{\Delta t} - \frac{L_3^-}{\mu_3} - \frac{1}{\mu_3} - k_{eC} - L_3^+\right\} \\ -L_3^+ & -L_3^+ & -L_3^+ & -L_3^+ & -L_3^+ & -L_3^+ & k_{reC} - L_3^+ \end{bmatrix}\Delta t,$$

$$D_8 = \begin{bmatrix} k_{eR} & 0 & 0 & 0 & 0 & 0 & 0 & \left\{\frac{1}{\Delta t} - k_{\deg R} - k_{reR}\right\} & 0 & 0 & 0 & 0 & 0 & 0 & 0 \end{bmatrix}\Delta t,$$

$$D_9 = \begin{bmatrix} 0 & k_{eR} & 0 & 0 & 0 & 0 & 0 & 0 & \left\{\frac{1}{\Delta t} - k_{\deg R} - k_{reR}\right\} & 0 & 0 & 0 & 0 & 0 & 0 \end{bmatrix}\Delta t,$$

$$D_{10} = \begin{bmatrix} 0 & 0 & k_{eR} & 0 & 0 & 0 & 0 & 0 & 0 & \left\{\frac{1}{\Delta t} - k_{\deg R} - k_{reR}\right\} & 0 & 0 & 0 & 0 & 0 \end{bmatrix}\Delta t,$$

$$D_{11} = \begin{bmatrix} 0 & 0 & 0 & k_{eR} & 0 & 0 & 0 & 0 & 0 & 0 & \left\{\frac{1}{\Delta t} - k_{\deg R} - k_{reR}\right\} & 0 & 0 & 0 & 0 \end{bmatrix}\Delta t,$$

$$D_{12} = \begin{bmatrix} -k_{eC} & -k_{eC} & -k_{eC} & -k_{eC} & -k_{eC} & -k_{eC} & -k_{eC} & -k_{eC} & -k_{eC} & -k_{eC} \\ -k_{eC} & \left\{\frac{1}{\Delta t} - k_{\deg C} - k_{reC} - k_{eC}\right\} & -k_{eC} & -k_{eC} & -k_{eC} \end{bmatrix}\Delta t,$$

$$D_{13} = \begin{bmatrix} 0 & 0 & 0 & 0 & k_{eC} & 0 & 0 & 0 & 0 & 0 & 0 & 0 & \left\{\frac{1}{\Delta t} - k_{\deg C} - k_{reC}\right\} & 0 & 0 \end{bmatrix}\Delta t,$$

$$D_{14} = \begin{bmatrix} 0 & 0 & 0 & 0 & 0 & k_{eC} & 0 & 0 & 0 & 0 & 0 & 0 & 0 & \left\{\frac{1}{\Delta t} - k_{\deg C} - k_{reC}\right\} & 0 \end{bmatrix}\Delta t,$$

$$D_{15} = \begin{bmatrix} 0 & 0 & 0 & 0 & 0 & 0 & k_{eC} & 0 & 0 & 0 & 0 & 0 & 0 & 0 & \left\{\frac{1}{\Delta t} - k_{\deg C} - k_{reC}\right\} \end{bmatrix}\Delta t.$$

Under stability conditions on the time step, the time dependent solution $u^{k+1} = Du^k + b$ may converge to the solution of the discrete steady state problem $u = Du + b$. We use the following theorem of Geometric Series for Matrices [24] and the definition of infinity norm [24] in order to find the steady-state solutions.

Theorem 1 (Geometric Series for Matrices). *Consider the scheme $u^{k+1} = Du^k + b$. If the infinity norm of D is less than one, then*

1. *$u^{k+1} = Du^k + b$ converges to $u = Du + b$,*
2. *$I - D$ has an inverse,*
3. *$I + \cdots + D^k$ converges to the inverse of $I - D$*

and the steady state solution is $u = (I - D)^{-1}b$.

We note that, based on this theorem, initial conditions are not involved in the determination of the steady-state solutions.

Definition 1. The infinity norm of the $n \times 1$ column vector $x = [x_i]$ is a real number

$$\|x\| \equiv \max_i | x_i | .$$

The infinity norm of an $n \times n$ matrix $D = [d_{ij}]$ is

$$\|D\| \equiv \max_i \sum_j | d_{ij} | .$$

We can conclude that for Eq. (2.40), the condition for convergence is $\|D\| \equiv \max_i \sum_j | d_{ij} | < 1$ and the steady-state solution is $u = (I - D)^{-1} b$.

3. Parameter estimation

3.1. Genetic algorithms (GAs): a tool for computational parameter optimization

Genetic algorithms (GAs) are probabilistic search techniques developed by Holland and his colleagues in 1975. GAs can evolve good optimum solutions by mimicking two biology mechanisms: natural selection and chromosome encoding [29,30]. In natural, organisms evolve by means of two primary processes: natural selection and sexual reproduction [30]. Natural selection determines which individuals in a population survive or die. Through natural selection, living organisms with a greater fitness to the environment have greater probability of surviving and reproducing. Sexual reproduction ensures genetic variation via genetic recombination among their offspring. These variations allow the organisms to evolve.

To adapt GAs to solve an optimization problem, candidate solutions need to be represented in form of GAs-string, called "chromosomes" (see Fig. 5). This example uses a binary code representation in which the solutions are then transformed and written as a string of bits, 0s or 1s. Then, a phenotype of an organism is evaluated by fitness function, a mathematical function used to measure how well the solution solves the problem. Mimicking two natural adaptation mechanisms including natural selection and chromosome encoding, GAs evolve solution to the problem by repeatedly modifying a population via three major GAs operators–selection, crossover, and mutation. Simulating natural selection, the selection operator is carried out to choose and reproduce the strings with high fitness scores while others are eliminated. The selected chromosomes are copied to create parent chromosomes. Then, crossover operation is applied into parent chromosomes. It combines segments of parent chromosomes to form two offspring. Crossover allows an exploitation of good characteristics (or the promise search space) determined by the parents. The last GA operator is mutation. Mutation alters one or more genes of a selected chromosome, by a random change with small chance. This operation introduces diversity into the population. The diversity of population could help avoid local optimum convergence of the algorithm. The iterative algorithm to evolve a solution to a problem on a computer could be summarized as follows (see Fig. 6):

(1) Population preparation;
(2) Fitness evaluation;
(3) Selection;
(4) Crossover and mutation.

Because of their simple and straightforward mechanism as mentioned earlier, GAs can be seen as a tool empowering researchers' competence in scientific investigation.

3.2. Genetic algorithm via MATLAB®

Although the logic of GAs is simple, applying GAs in practice involves many programming tasks. This programming may be seen as an obstacle for students who lack of experience with them. Fortunately, present technologies have provided powerful tools to aid researchers and educators.

3.2.1. MATLAB®

MATLAB® (matrix laboratory) is a software package for numerical matrix computations. It provides a friendly interactive environment that enables students to use it at many levels, from simple to advanced calculations. It contains advanced tools for technical computing such as algorithm development, data visualization, and mathematical function, e.g., data analysis, statistics, linear algebra, numeric integration, and optimization.

3.2.2. Genetic algorithm tool

Genetic algorithm tool (gatool) is an optimization tool using GAs provide by MATLAB®. It can be accessed through a graphical user interface (GUI) or the MATLAB® command line. GUIs let users quickly and conveniently define a problem and set various algorithm options to fine-tune the optimization, while the command line allows users to modify or create

their own custom functions. In addition, it provides a number of plotting functions for run time visualization that gives feedback about the optimization. To open the tool, enter

$\gg$ *gatool*

at the MATLAB® prompt.

3.3. Genetic algorithm parameter optimization implementation

In the current paper, the optimization problem consists of the estimation of 21 parameters of our ordinary differential equation model, formed by Eqs. (2.45), (2.46) and (2.49) that describe the variation of numbers of active G-proteins (which correspond to the responses to the agonist concentration). The parameters consist of $L_j^+, L_j^-, \mu_j, k_j^+, K^+, k_{gtp}, G_{\beta\gamma}, V, k_{eR}, k_{reR}, k_{\deg R}, k_{eC}$, k_{reC} and $k_{\deg C}$, when $j = 1,2,3$. In order to determine the optimal values of these parameters, we have to minimize a weighted distance measure J between experimental and predicted values of state variables, represented by the vector y [23]:

$$J = \sum_{j=1}^{m} \sum_{i=1}^{n} w_{ij}\{[y_{pred}(i) - y_{\exp}(i)]_j\}^2, \tag{2.50}$$

where the entries of vector y represent values of the steady state activated G-proteins concentration, n is the number of data points for each experiment, m is the number of G-protein subtypes, $y_{\exp}$ represents the known experimental data, and y_{pred} is the vector of states that corresponds to the predicted theoretical evolution using the model with a given set of the 21 parameters. Furthermore, w_{ij} corresponds to the different weights taken to normalize the contributions of each term. Here we let $w_{ij} = \{1/[y_{\exp}(i)]_j\}^2$.

In this study, we use the genetic algorithm approach to estimate the values of the model parameters. Genetic algorithm tool (a graphical user interface) in MATLAB has been applied for this purpose. Eq. (2.50) gives a fitness function that we want to minimize. In this optimization scheme, there are two constrains. One is required for the steady-state, that is, the infinity norm of D being less than one, and the other, that assists in finding functional minima faster, is the bounds of the variables. Based on biological data and our previous estimations, we set the ranges, within which our variables are allowed to vary as given in the following.

L_j^+	L_j^-	μ_j	k_j^+	K^+	$k_{gtp}G_{\beta\gamma}$	V	$k_{eR}, k_{reR}, k_{\deg\ R}, k_{eC}, k_{reC}, k_{\deg\ C}$
0.05-20	5-1500	1-2500	0.01-100	0.001-10	0.01-100	0-1	0-2500

We assume that the numbers of all G-protein subtypes are equal (that is nondimensionalized $g_1 = g_2 = g_3 = 1/3$) and the concentration ratio of the receptors and G-proteins ($N = R_0/G_0$) equals 1. In order to estimate the parameters, we use the experimental results of Cordeaux et al. [13] concerning the effect of the agonist NECA and CPA, acting on adenosine A_1 recep-

Table 1
The values of the model parameters for NECA and CPA.

Parameter	NECA	CPA
L_1^+	10.8576	19.9677
L_2^+	6.9852	12.7865
L_3^+	0.0737	1.0099
L_1^-	1499.9997	1399.4590
L_2^-	1062.9664	1147.0858
L_3^-	824.2943	1221.9734
μ_1	2499.9533	2197.6745
μ_2	911.0545	63.9351
μ_3	217.7341	21.8868
k_1^+	99.9858	99.9842
k_2^+	69.3132	33.9221
k_3^+	4.1467	0.3783
K^+	0.6160	4.1654
$k_{gtp}G_{\beta\gamma}$	23.7822	13.3884
V	0.9993	0.6555
k_{eR}	159.6044	53.8139
k_{reR}	2499.8288	2079.3102
$k_{deg\ R}$	15.9061	17.0189
k_{eC}	294.2709	424.2536
k_{reC}	2448.4638	2256.6692
$k_{deg\ C}$	484.6408	2005.1535

tors, on the activation of G_i,G_s and G_q(for more information about G-protein pathways, see [25]). Note that the subscripts i,s and q identify different G-protein families, each regulating specific classes of effector molecules within the cell.

4. Results and discussion

All the computations were performed in MATLAB using a PC/Pentium (1.73 GHz) platform running Windows XP 2002. We want to minimize the fitness function (J) in Eq. (2.50) meaning that we have to find three steady state activated G-proteins concentrations for each G-protein subtypes that minimize J. The minimum results of fitness function are 1.0457×10^{-5} for NECA agonists and 7.9581×10^{-6} for CPA, obtained after a total computation time of 3.55 h for each result of fitness function, when we set population size = 60 and running for 200 generations in this GA optimization. The size of population is parameters.

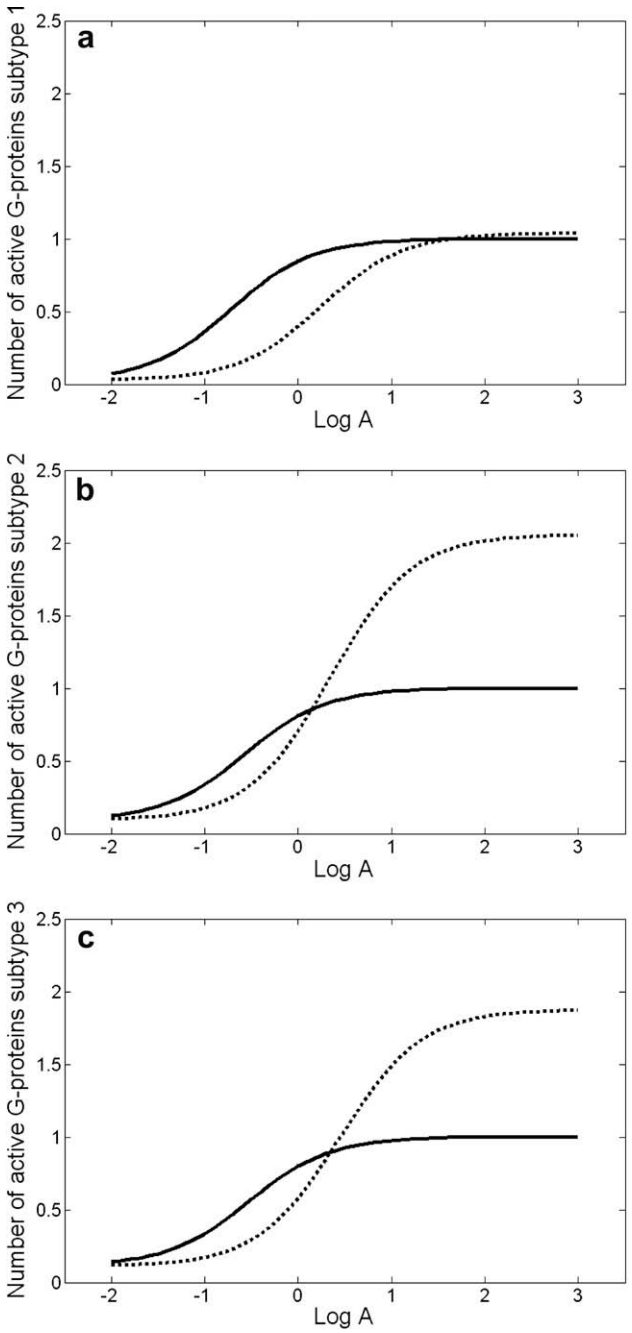

Fig. 3. Prediction of the effect of NECA (dashed line) and CPA (solid line), given relative to the maximum response of CPA, on G-protein activation for (a) $G_i = G_1$; (b) $G_q = G_2$; (c) $G_s = G_3$. Parameter values are given in Table 1 with $g_1 = g_2 = g_3 = 1/3$ and $N = 1$ for both drugs.

Setting the population size too small may yield premature convergence of GAs. While, setting the large size of population remains the population variety that could enable GAs to search more point and thereby prevent local optimum trapping of the algorithms. However, the time used for a population improvement might be too long for the large population size. To optimal population size, an experiment is conducted to study the effect of population size on GAs performance. In this experiment, the population size is set to 10, 20 (default), 30, 40 and 50. We obtained the estimated parameters according to Table 1.

To verify the validity of the model and the results obtained so far, we now attempt qualitatively reproduce the experimental results of Cordeaux et al. [13]. We set $G_i = G_1$, $G_q = G_2$, $G_s = G_3$ with $g_1 = g_2 = g_3 = 1/3$ and $N = 1$ for both drugs – NECA and CPA, and the other parameter values are set as expressed in Table 1. The comparison of G-protein activation by these two agonists representing the effect of the agonists NECA and CPA on the activation of G subtype 1, 2, and 3 is depicted in Fig. 3. It was found that except G subtype 1, NECA appeared to be a more efficacious drug than CPA. On contrary, when we consider the minimum doses of agonists required for the effectors (use G^*'s as indicators) to reach the maximum, the results signify that CPA was more potent than NECA. In other words, in terms of drug efficacy NECA agonists seem to be more effective drug than CPA when they were linked with pathways associated with G subtype 2 and 3. The results are in good qualitative agreement with the responses recorded by Cordeaux et al. [13], on the effect of NECA and CPA on $[^{35}S]GTP_\gamma S$ binding to $G\alpha_{i(1-3)}$, $G\alpha_{Q/11}$ and $G\alpha_S$ (in their Fig. 9).

The model parameters allow us to obtain qualitative insight into the likely governing mechanisms and their interactions. The values of μ_1, μ_2 and μ_3, signifying the effect and preference of drugs for the different pathways, which yield $\mu_1 > \mu_2, \mu_3$ for both NECA and CPA, infer that both agonists prefer the G_1- (that is G_i-) linked pathway, which means that the available receptors will be preferentially channeled to bind with the G_i before the others. In addition, the parameters for receptor and G-protein association (k_j^+) with $k_1^+ > k_2^+, k_3^+$ indicates that the association of active receptors type 1 (R^{1*}, R_A^{1*}) with their

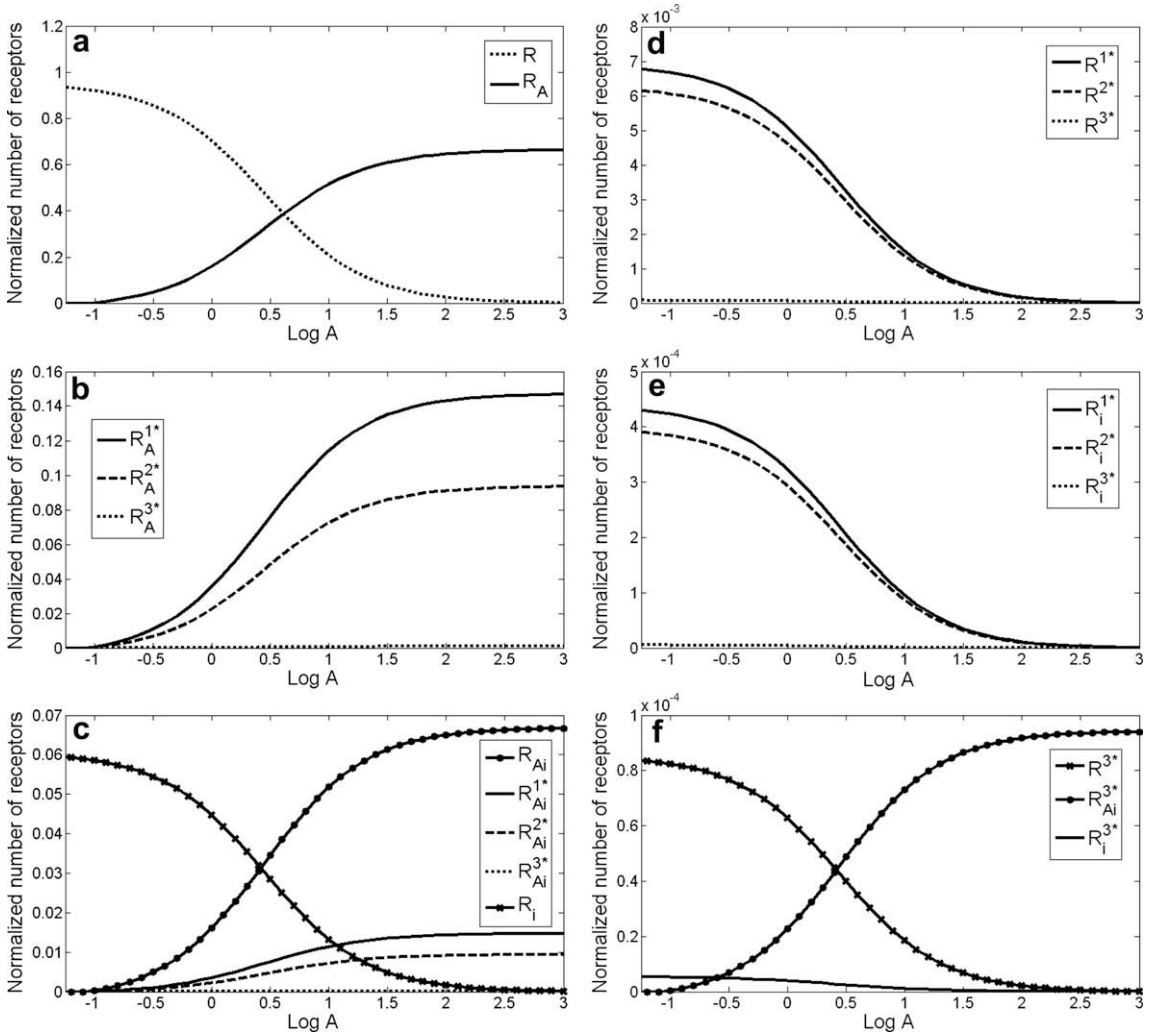

Fig. 4. Prediction of the effect of NECA agonist concentration, given relative to the total number of all types of receptors in the system ($R_{total} = 1$), on number of each type of receptors. Parameter values are given in Table 1 with $g_1 = g_2 = g_3 = 1/3$ and $N = 1$.

specific G-protein subtype is greater than that of the other receptor type, which leads to the more active G-protein subtype1 (G_1^*). For simplicity, the values of L_j^+ and L_j^- (when $j = 1,2,3$) can be analyzed in terms of $L_j = L_j^-/L_j^+$ (which has appeared in [3]). With our estimated parameter values, we obtain $L_1 = 138.1521$, $L_2 = 152.1741$ and $L_3 = 11184.45$ for NECA, and $L_1 = 70.0861$, $L_2 = 89.7107$ and $L_3 = 1209.9945$ for CPA. We can see that $L_3 \gg L_1, L_2$. This means that, at the steady-state, the expression of active state R^{3^*} is much lower than R^{1^*} and R^{2^*}. From Table 1, $k_{eC} > k_{eR}$ for both agonists, from which it can be deduced that the agonists stimulate internalization of GPCRs – adenosine A_1 receptors. This hypothesis is consistent with many other earlier experimental results about internalization of GPCRs (reviewed by [26]) especially the experiments on adenosine A_1 receptors [27,28]. Similarly, for degradation, the rate constant $k_{\deg C} > k_{\deg R}$, which leads us to suppose that the ligands also induce degradation of adenosine A_1 receptors. However, due to the values of recycling rate constants, $k_{reC} \approx k_{reR}$, we hypothesize that ligands are not involved in recycling of the receptors.

In order to get insights into the dynamics of GPCRs, we find the steady-state value of each type of receptors using values of our model parameters as given in Table 1, and then illustrate the dependence of the number of each type of receptors on the agonist, the concentration of which is considered here only for NECA (Fig. 4).

Fig. 4a shows that the number of receptor/ligand complexes (R_A) increases with A as more agonists become available to bind with free receptors and saturates when all the free receptors (R) in the system is bound. Because some of the receptor/ligand complexes (R_A) are transformed into other receptor states, that is the greatest contribution to the result that the maximum number of receptor/ligand complexes (R_A) is not equal to that of the free receptors (R) which appear when the system is exposed to very low concentration of agonists. In the same way, the numbers of other complex states $R_A^{j^*}, R_{Ai}$ and $R_{Ai}^{j^*}$ (when $j = 1,2,3$) also rise as agonist concentration (A) increases (see Fig. 4b and c). The numbers R, R^{j^*}, R_i and $R_i^{j^*}$ (when $j = 1,2,3$) decline while agonist concentration (A) is on the increase (see Fig. 4c–e). The reason why R and R^{j^*} decrease is that when agonists exist in the system, they tend to bind with free receptors which leads to the conversion of R and R^{j^*} into R_A and $R_A^{j^*}$. Therefore, the more agonists are present, the less R and R^{j^*} are. The effect of agonist concentration on internalization of active and inactive free receptors (R_i and $R_i^{j^*}$) can be explained by the fact that free receptors (R and R^{j^*}) remaining in the system, exposed to high concentration of agonists, are so few that few receptors can be internalized to become the states R_i and $R_i^{j^*}$. Regarding the order of magnitude of the receptor numbers as shown on Y-axis, we can see that the value of R_i is more than that of $R_i^{j^*}$. The reason for this is that the number of inactive free receptors (R) is much higher than that of active free receptors (R^{j^*}) in the system. This means that there are much more available inactive receptors to be internalized than active free receptors. However, the fact that $R > R^{j^*}$ can not be seen directly from Fig. 4 due to the limitation of plotting the numbers of receptors which are of wildly different orders of magnitude.

In order to know the proportions of each receptor type, we display the amounts of each state of receptors at steady-state when exposed to agonists at one value of concentration (as shown in Table 2).

The numbers of receptors in this table can help to visualize receptor trafficking and the range of possible behavior. The sequences of receptor types are ranked based on their numbers from the maximum to the minimum as follows: $R_A, R, R_A^{1^*}, R_A^{2^*}, R_{Ai}, R_i, R_{Ai}^{1^*}, R_{Ai}^{2^*}, R^{1^*}, R^{2^*}, R_A^{3^*}, R_i^{1^*}, R_i^{2^*}, R_{Ai}^{3^*}, R^{3^*}, R_i^{3^*}$ for NECA and $R_A, R_A^{1^*}, R_{Ai}, R_A^{2^*}, R, R_{Ai}^{1^*}, R_{Ai}^{2^*}, R_A^{3^*}, R_i, R^{1^*}, R^{2^*}, R_{Ai}^{3^*}, R^{3^*}, R_i^{1^*}, R_i^{2^*}, R_i^{3^*}$ for CPA. These orders can be analyzed as follow. When both agonists ($A = 10$) are present in the system, R_A is greatly induced. R_A then is mostly transformed into $R_A^{1^*}, R_A^{2^*}, R_{Ai}$ which results in these three states being present at great amounts in the system. The reason that the value of $R_A^{1^*}$ is greater than $R_A^{2^*}$ is $L_1^+ > L_2^+$ and $\mu_1 > \mu_2$. $L_1^+ > L_2^+$ means that the inactive receptors type 1 are converted into an active state more rapidly than that of type 2. As for μ, the higher its value is, the smaller the backward conversion rate L_j^-/μ_j from $R_A^{j^*}$ to R_A becomes. Regarding the L_j value that represents the ratio of rate constant of converting R^{j^*} into R to that of R into R^{j^*}, $L_3 > L_2 > L_1$ can explain the phenomenon of the numbers of active receptors that $R^{1^*} > R^{2^*} > R^{3^*}$. Moreover, $R_{Ai}^{j^*} > R_i^{j^*}$ when $i = 1,2,3$, consistent with the result that internalization rate constant of receptor/ligand complexes is higher than that of free receptors ($k_{eC} > k_{eR}$). The number of inactive complexes (R_A) for the CPA activated system is higher than that for NECA because K^+ of CPA is bigger than K^+ of NECA. (K^+ represents the rate constant of receptor/ligand association).

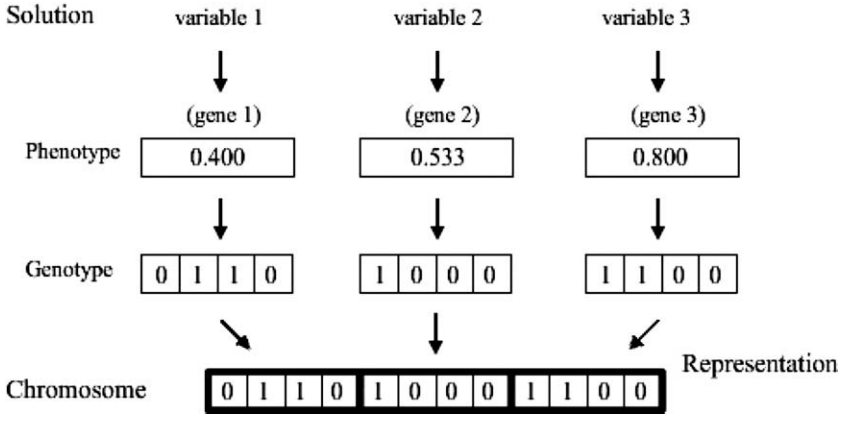

Fig. 5. The process of GAs string representation of the three parameters.

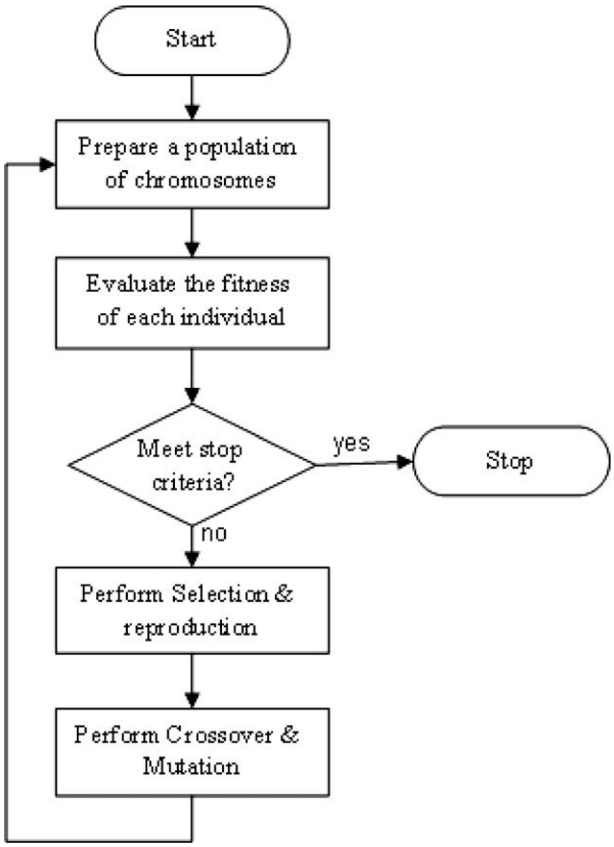

Fig. 6. Flowchart of simple genetic algorithm.

Table 2
The numbers of receptors at steady-state when exposed to NECA and CPA of which nondimensionalized concentration (A) are equal to 10. Data have been expressed as percentages (%) of the total number of receptors in each system.

Parameter	NECA	CPA
R	20.8629	3.2708
R^{1^*}	0.1503	0.0453
R^{2^*}	0.1362	0.0352
R^{3^*}	0.0018	0.0026
$R_A^{1^*}$	11.4186	7.5412
$R_A^{2^*}$	7.2673	4.4458
$R_A^{3^*}$	0.0729	0.2990
R_{Ai}	5.1850	7.5190
$R_{Ai}^{1^*}$	1.1456	0.7507
$R_{Ai}^{2^*}$	0.7291	0.4426
$R_{Ai}^{3^*}$	0.0073	0.0298
R_i	1.3236	0.0840
$R_i^{1^*}$	0.0095	0.0012
$R_i^{2^*}$	0.0086	0.0009
$R_i^{3^*}$	0.0001	0.0001
R_A	51.6811	75.5319

Table 3
The numbers of active G-protein subtypes at steady-state in the systems exposed to NECA and CPA of which nondimensionalized concentration (A) are equal to 10. Data have been expressed as percentages (%) of the total number of G-proteins in each system. ($G_{total} = G_1^* + G_2^* + G_3^* + G_1 + G_2 + G_3 = 100\%$).

Parameter	NECA	CPA
G_1^*	10.9075	12.0553
G_2^*	5.9160	3.3987
G_3^*	0.0043	0.0028

The proportions of each active G-protein types at steady-state when exposed to agonists at one concentration value are shown in Table 3. We explain these proportions by considering the value of k_j^+. From Table 1, $k_1^+ > k_2^+ > k_3^+$ for both agonists. k_j^+ is the rate constant for coupling of activated receptors type j and inactive G-proteins type j that leads to activation of G-proteins. Therefore, the higher is the value of the k_j^+, then the higher is the number of active G-protein type j, which can explain why $G_1^* > G_2^* > G_3^*$.

5. Conclusion

Under normal physiological conditions, many dynamic trafficking events of GPCRs occur in the signal transduction process concurrently with the receptor binding [10]. These dynamic trafficking events are usually classified into four groups; internalization, recycling, degradation and synthesis. Of all GPCR activity and regulation, the internalization or sequestration of agonist-activated receptors into the intracellular membrane compartments of the cell has become the subject of intensive investigation over the past several years [26]. However, qualitative studies of internalization and the other dynamic trafficking events of GPCRs are more difficult than that of surface receptor/ligand binding because the molecular species must be followed as they move through various cellular organelles. Due to this fact, mathematical modeling plays an important role in studying these trafficking processes.

In this study, we build on the model of Chen et al. [3] and propose a mathematical model to investigate the dynamics of GPCRs, basing our model on the possibility of agonist-directed trafficking, allowing the constitutive activities in the absence of any ligand, and three assumptions that the distribution of receptors and G-proteins is uniform throughout, G-protein activation is considered as a one-step process, and receptor trafficking rate constants for each conformation state of free receptor and complexes are equal. By using genetic algorithm and the experimental results obtained by Cordeaux et al. [13], we obtain approximate values of model parameters (see Table 1) which helps us to gain a better understanding of the dynamics of GPCRs. Moreover, these parameters are also used to find steady-state levels of all types of G-proteins and receptors. The steady-state levels of the activated G-proteins are depicted in Fig. 3, consistent with experimental data [13] on the activation of individual G-protein using [^{35}S]GTPγS binding. The numbers of receptors are shown in Fig. 4 and Table 2 in order to obtain insights into receptor trafficking. In addition, all these solutions confirm that agonists (NECA and CPA) stimulate internalization of GPCRs (adenosine A_1 receptors) and lead us to two hypotheses. The first is that NECA and CPA also induce degradation of adenosine A_1 receptors. The second is that recycling of adenosine A_1 receptors is independent from the existing agonists. We hope that this study provides a basis for reliable production and analysis of agonist pharmacology within systems of promiscuous multiple effector pathways.

Lastly, we are now on the process of interpretating these obtained optimized parameters. With more understanding their biological meanings and implications, it would provide us more confidence or a way to better or adjust our model. In addition, since there are a large numbers of parameters (21 parameters) to deal with, it may be helpful if we can improve our numerical algorithm to get better the computational times. Once these all mentioned factors are optimized, we believe that the study of time-dependent problem corresponding to this work would be very interesting and benefit other researchers.

Acknowledgements

We are grateful to anonymous referee for helpful comments and raising interesting questions resulting in great improvement of our paper. This work was supported by the National Center for Genetic Engineering and Biotechnology (BIOTEC), the Thailand Research Fund (TRF), the Commission on Higher Education, and the Thailand Center of Excellence in Physics (research project in integrated physics).

References

[1] A. Persidis, Signal transduction as a drug-discovery platform, Nat. Biotech. 6 (11) (1998) 1082–1083.
[2] N.A. Campbell, J.B. Reece, Biology, seventh ed., Benjamin Cummings, San Francisco, 2005.
[3] C.Y. Chen et al., Modelling of signalling via G-protein coupled receptors: pathway-dependent agonist potency and efficacy, Bull. Math. Biol. 65 (5) (2003) 933–958.
[4] S.H.P. Paul et al., Oligomerization of G protein-coupled receptors: past, present, and future, Biochemistry 43 (50) (2004) 15643–15656.
[5] S.J. Hill, G-protein-coupled receptors: past, present and future, Br. J. Pharmacol. 147 (Suppl. 1) (2006) S27–S37.
[6] D. Filmore, It's a GPCR world, Mod. Drug Discov. 7 (11) (2004) 2002–2005.
[7] W.M. Becker, The World of the Cell, fourth ed., Benjamin Cummings, San Francisco, 2000.
[8] E.J. Neer, Heterotrimeric G proteins: organizers of transmembrane signals, Cell 80 (2) (1995) 249–257.
[9] A. Surya, J.M. Stadel, B.E. Knox, Evidence for multiple, biochemically distinguishable states in the G protein-coupled receptor, rhodopsin, Trends Pharmacol. Sci. 19 (7) (1998) 243–247.
[10] D.A. Lauffenburger, J.J. Linderman, Receptors: Models for Binding, Trafficking, and Signaling, Oxford University Press, New York, 1993.
[11] A. De Lean, J.M. Stadel, R.J. Lefkowitz, A ternary complex model explains the agonist-specific binding properties of the adenylate cyclase-coupled beta-adrenergic receptor, J. Biol. Chem. 255 (15) (1980) 7108–7117.
[12] R. Seifert, K. Wenzel-Seifert, Constitutive activity of G-protein-coupled receptors: cause of disease and common property of wild-type receptors, Naunyn-Schmiedeberg's Arch. Pharmacol. 366 (5) (2002) 381–416.
[13] Y. Cordeaux et al., Influence of receptor number on functional responses elicited by agonists acting at the human adenosine A(1) receptor: evidence for signaling pathway-dependent changes in agonist potency and relative intrinsic activity, Mol. Pharmacol. 58 (5) (2000) 1075–1084.
[14] P. Samama et al., A mutation-induced activated state of the beta 2-adrenergic receptor. Extending the ternary complex model, J. Biol. Chem. 268 (7) (1993) 4625–4636.

[15] J.M. Weiss et al., The cubic ternary complex receptor-occupancy model I. Model description, J. Theoret. Biol. 178 (2) (1996) 151–167.
[16] J.M. Weiss et al., The cubic ternary complex receptor-occupancy model II. Understanding apparent affinity, J. Theoret. Biol. 178 (2) (1996) 169–182.
[17] S. Tucek, P. Michal, V. Vlachov, Modelling the consequences of receptor-G-protein promiscuity, Trends Pharmacol. Sci. 23 (4) (2002) 171–176.
[18] K.A. Berg et al., RNA-editing of the 5-HT 2C receptor alters agonist–receptor–effector coupling specificity, Brit. J. Pharmacol. 134 (2001) 386–392.
[19] P. Leff et al., A three-state receptor model of agonist action, Trends Pharmacol. Sci. 18 (10) (1997) 355–362.
[20] T.A. Riccobene, G.M. Omann, J.J. Linderman, Modeling activation and desensitization of G-protein coupled receptors provides insight into ligand efficacy, J. Theoret. Biol. 200 (2) (1999) 207–222.
[21] J. Nocedal, S.J. Wright, Numerical Optimization, second ed., Springer Series in Operations Research, Springer, New York, 2006.
[22] D.E. Goldberg, Genetic Algorithms in Search, Optimization, and Machine Learning, first ed., Reading: Addison-Wesley Professional, 1989.
[23] C.G. Moles, P. Mendes, J.R. Banga, Parameter estimation in biochemical pathways: a comparison of global optimization methods, Genom. Res. 13 (11) (2003) 2467–2474.
[24] R.E. Write, Computational Mathematics: Models, Methods and Analysis with MATLAB and MPI, Chapman & Hall/CRC, Boca Raton, 2003.
[25] S.R. Neves, P.T. Ram, R. Iyengar, G protein pathways, Science 296 (5573) (2002) 1636–1639.
[26] S.S. Ferguson, Evolving concepts in G protein-coupled receptor endocytosis: the role in receptor desensitization and signaling, Pharmacol. Rev. 53 (1) (2001) 1–24.
[27] M. Escriche et al., Ligand-induced caveolae-mediated internalization of A1 adenosine receptors: morphological evidence of endosomal sorting and receptor recycling, Experim. Cell Res. 285 (1) (2003) 72–90.
[28] S. Gines et al., Involvement of Caveolin in ligand-induced recruitment and internalization of A1 adenosine receptor and adenosine deaminase in an epithelial cell line, Mol. Pharmacol. 59 (5) (2001) 1314–1323.
[29] J.W. Chinneck, Practical Optimization: A Gentle Introduction, 2003. <http://www.sce.carleton.ca/faculty/chinneck/po.html>.
[30] J.H. Holland, Genetic Algorithms, Scientific American, 1992. pp. 44–50.